J Mater Sci (2008) 43:6260–6266
DOI 10.1007/s10853-008-2909-2

Achieving high strain rate superplasticity via severe plastic deformation processing

Chih-Fu Yang · Jiun-Hung Pan · Ming-Chieh Chuang

Received: 26 January 2008 / Accepted: 28 July 2008 / Published online: 13 August 2008

Abstract In this study, a thermomechanical process consisting of general precipitation and severe plastic deformation through equal channel angular extrusion (ECAE) was applied to a Zn-22 wt.% Al alloy to produce a microduplex structure for high strain rate (HSR) superplasticity studies. Microstructures, hardness, and superplastic properties of the Zn–Al alloy were studied by using differential scanning calorimetry (DSC), scanning electron microscopy (SEM), recordable hydraulic press, and a tensile test with a hot stage. A work-softening phenomenon due to the occurrence of a grain boundary-sensitive dynamic recrystallization (DRX) was observed during the ECAE processing of the Zn–Al alloy at the extrusion temperatures investigated from −10 °C to 50 °C. An important discovery regarding the grain boundary-sensitive DRV was realized in this study such that through a progressive work-softening process the Zn–Al alloy will eventually exhibit HSR superplastic properties.

Introduction

Fine-grained dual-phase Zn-22 wt.% Al alloy is a superplastic material that is capable of exhibiting exceptionally high tensile ductility (>1,000%) over a limited range of strain rates and temperatures. Typically, high elongations attained in this alloy are at low strain rates in the vicinity of 10^{-3}–10^{-5} s^{-1}. Recently, high strain rate (HSR) superplasticity [1–5] in ultra-fine-grained materials has attracted great interest for its great potential in engineering applications. In addition to the high speed superplastic forming of sheet alloys, commercial applications of high speed superplastic forging are expected to lead to high productivity in the fabrication of products with complicated shapes in the near future, although there are currently few commercial applications of superplastic forging.

Although the grain boundary sliding mechanism for the high temperature (HT) low strain rate (LSR) superplasticity has been recognized and extensively studied, a comprehensive investigation of the controlling mechanism for HSR superplasticity has not yet been conducted. As such, this research aims to explore the governing mechanism of HSR superplasticity by using a Zn-22 wt.% Al alloy. A special thermomechanical process, consisting of general precipitation and severe plastic deformation (SPD) [6, 7] through an equal channel angular extrusion (ECAE) [8, 9], was designed and applied to the Zn–Al alloy to produce a microduplex structure with HSR superplasticity capability.

Experimental procedures

The Zn-22 wt.% Al alloy used in this study was prepared by melting proper amounts of 99.7% purity Al and 99.99% purity Zn in a graphite crucible in air and casting into 450 mm × 300 mm × 35 mm blocks. After homogenization at 380 °C for 48 h, these castings were hot rolled and sectioned to 16 mm × 16 mm square bars for further thermomechanical treatment. The thermomechanical treatment applied to the Zn–Al alloy bars consists of: (i) solid solutioning at 380 °C for 1 h, quench, and then either a 1-step aging (−10 °C/24 h in alcohol) or a 2-step aging (−10 °C/24 h in alcohol and 250 °C/24 h in an oil bath) to produce, respectively, a sub-micron or a micron scale grain

C.-F. Yang (✉) · J.-H. Pan · M.-C. Chuang
Department of Materials Engineering, Tatung University,
40 ChungShan North Road, 3rd Sec., Taipei 10451,
Taiwan, ROC
e-mail: cfuyang@ttu.edu.tw

structure and (ii) mechanical deformation via ECAE to work soften the Zn–Al alloy, eventually leading to HSR superplasticity.

The ECAE was performed using an extrusion die designed to yield a shear strain of 1.05 by each pass. The inner contact angle and the arc of curvature at the outer point of contact between the inlet and outlet channels of the die are 90° and 20°, respectively. Zn–Al alloy bars were extruded under a variety of conditions, including extrusion speeds of 10 and 90 mm/min, extrusion temperatures of 10 °C, room temperature (RT), and 50 °C, and various extrusion strains (up to 8 passes) by using ECAE route C [10].

For microstructural examination, the Zn-22 wt.% Al alloy specimens, in various stages of processing, were ground to 1000-grit finish and polished through 0.05 μm Al_2O_3 powders, and then examined using a JEOL 5600 scanning electron microscope (SEM). Thermal analysis of the dual-phase Zn-22 wt.% Al alloy, in conjunction with a pseudo-single α phase Zn-95 wt.% Al and a pseudo-single β phase Zn-1 wt.% Al alloys for references, was performed using a TA Instrument 2910 differential scanning calorimeter (DSC) equipped with a modulated frequency thermal analyzer system of 910 DSC cell. For DSC measurement a small piece of wrought alloy, weighing about 10 mg, was cooled to 77 K in liquid nitrogen and then quickly cold rolled in air resulting in a 60% or greater reduction in thickness. To minimize the RT annealing effect after cold work, the DSC specimen was kept in liquid N_2 prior to the thermal analysis. The DSC measurement was carried out in high purity argon from −50 °C to 150 °C with a ramp speed of 10 °C/min. Microhardness of the Zn–Al alloy specimens was measured by using a Future-Tech FM-7 Vickers testing machine with a 50 g applied load for 10 s. The superplasticity of the Zn–Al alloy in various thermomechanical treated conditions was tested on a Hung-Ta HT8150 materials test system where the tensile strengths and elongations of specimens were tested at RT and 250 °C under a range of strain rates from 1×10^{-3} to 1×10^{-1} s^{-1} under a constant crosshead speed condition.

Results and discussion

DSC measurement

The result of the DSC measurement of the cold-worked dual-phase Zn-22 wt.% Al alloy is shown in Fig. 1. As can be seen in the figure, there is a distinct exothermic peak at −7.5 °C in the heating cycle of the cold-worked Zn–Al alloy specimen. By comparing this exothermic peak temperature of the Zn-22 wt.% Al alloy to those of the α-phase Zn-95 wt.% Al alloy (337 °C) and the β-phase Zn-1 wt.% Al alloy (−12 °C), it was confirmed that the exothermic peak of the dual-phase Zn-22 wt.% Al alloy is associated with the recrystallization of the zinc-rich β phase, but not the Al-rich α phase. The sub-zero recrystallization temperature of the β phase has a great impact on the RT mechanical behaviors of the wrought Zn–Al alloy since dynamic recovery (DRV), dynamic recrystallization (DRX), static recovery (SRV), and static recrystallization (SRX) are bound to take place to soften the alloy during "hot working" at RT. Similar work-softening phenomenon at RT was reported by Staszewski et al. [11] in which the hardness increased first with deformation and then decreased with further deformation in pure Zn and several dilute Zn alloys.

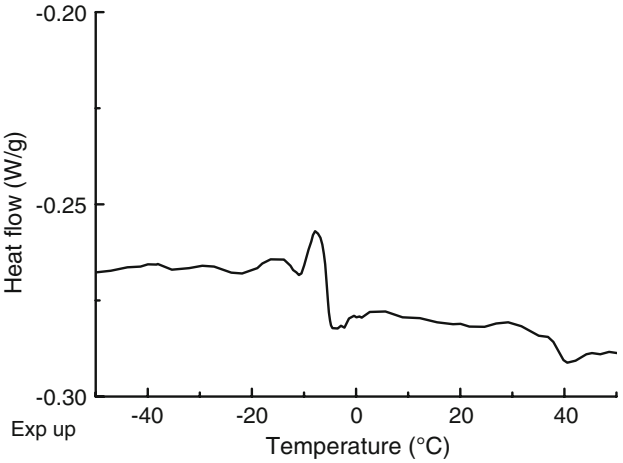

Fig. 1 DSC curve of a cold-worked Zn-22 wt.% Al alloy

Work-softening and anneal-hardening

Microstructures of the Zn–Al alloy in the 1-step aged (−10 °C/24 h) condition and those after ECAE (8 passes) at −10 °C, RT, and 50 °C are shown in Fig. 2. As can be seen in Fig. 2a, after solid solutioning, quench, and aging at −10 °C for 24 h, the Zn–Al alloy is composed of a mixture of approximately 40% unresolved supersaturated α′ phase and 60% mixtures of Al-rich α (dark grain) and Zn-rich β (white grain) precipitates. It was observed in the experiment that the retained α′ transformed completely to α and β precipitates after ECAE (4 passes) at −10 °C or 1 pass at 50 °C. It was also noted that after several passes of ECAE, the Zn–Al alloy started to release a great deal of heat. This indicates that exothermal reactions of DRV and/or DRX must have taken place in the course of ECAE at −10 °C, RT, and 50 °C so that a portion of the Zn–Al alloy can retain a near equiaxed grain structure after deformation. From Fig. 2b, c and d, the average grain size found after 8 passes of ECAE at −10 °C, RT, and 50 °C are about 0.3, 0.5, and 0.8 μm, respectively.

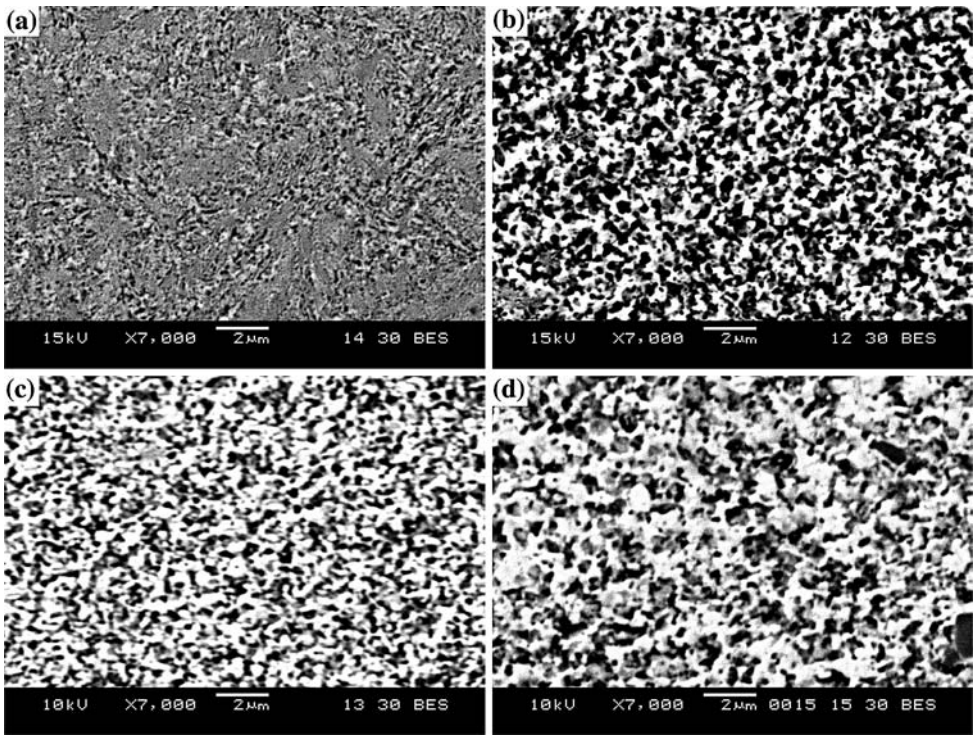

Fig. 2 Zn-22 wt.% Al (**a**) as 1-step aged (−10 °C/24 h), (**b–d**) after ECAE for 8 passes at −10 °C, RT, and 50 °C, respectively

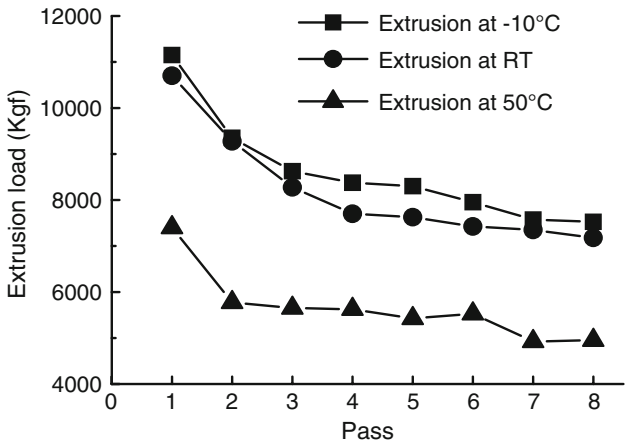

Fig. 3 Extrusion load versus ECAE pass for 1-step aged Zn–Al alloy specimens

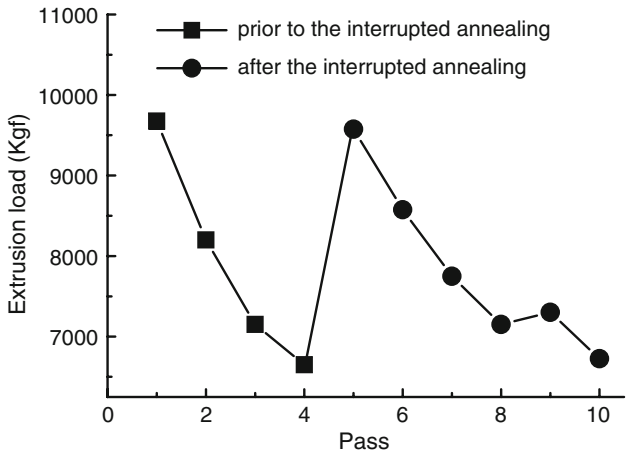

Fig. 4 Effect of an interrupted annealing (250 °C/30 min) on extrusion load of a Zn-22 wt.% Al alloy. The static annealing was carried out after the fourth ECAE pass

As can be seen in Fig. 3, the extrusion load of the Zn–Al alloy decreases monotonically with the number of ECAE passes regardless of the extrusion temperature. Possible reasons for this work-softening behavior to occur in the Zn–Al alloy include: (i) the phase transformation-induced lattice softening and (ii) the DRV/DRX-induced softening. In order to identify the exact mechanism governing the work-softening, an interrupted ECAE experiment was designed and carried out, in which an intermediate anneal treatment was applied to the Zn–Al alloy in the middle of repeated ECAE processing.

The procedures of the interrupted ECAE experiment include: (i) an initial 4-pass ECAE at −10 °C, (ii) an intermediate annealing at 250 °C for 30 min, and (iii) another 6-pass ECAE at −10 °C. The variation of extrusion load with pass in the interrupted ECAE experiment is shown in Fig. 4. This figure clearly shows the occurrence of a work-softening phenomenon in both the initial 4-pass and the later 6-pass ECAE, and in addition, it shows an anneal-hardening phenomenon by the intermediate anneal treatment. It was noted that after the intermediate annealing, the extrusion load of the annealed Zn–Al alloy resumes the value of its as-aged (undeformed) condition.

SEM micrographs of the Zn–Al alloy in various stages of the interrupted ECAE experiment, including the 1-step

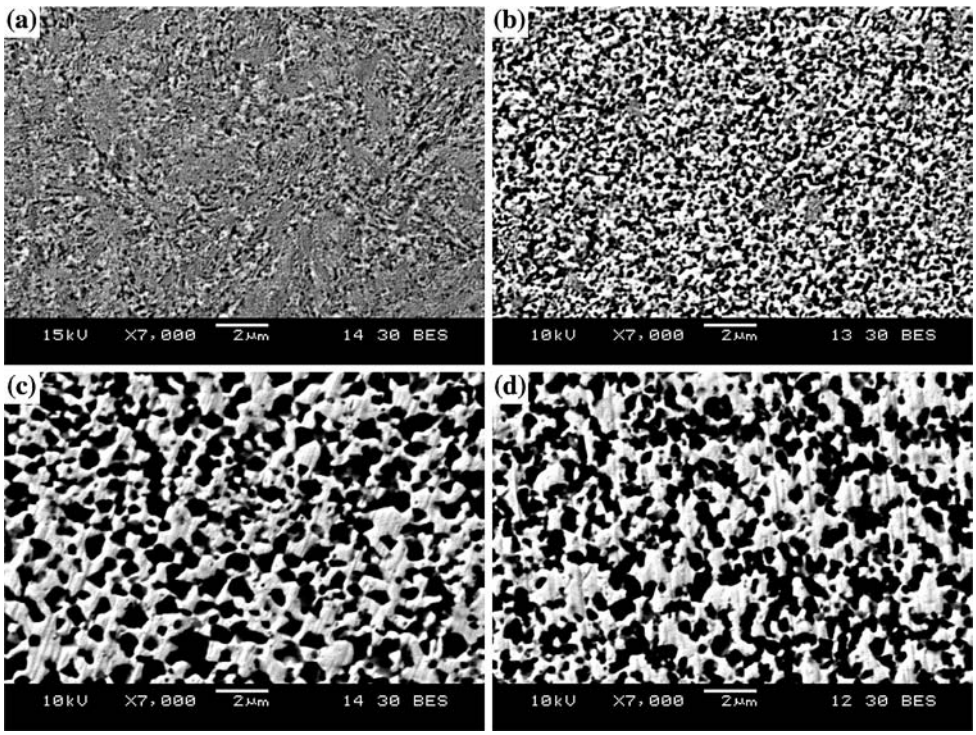

Fig. 5 Zn-22 wt.% Al (**a**) 1-step aged (−10 °C/24 h), (**b**) after 4 passes of ECAE at −10 °C, (**c**) interrupted annealed (250 °C/30 min), and (**d**) after the interrupted annealing and additional 6 passes of ECAE at −10 °C

aged, after ECAE for 4 passes, after intermediate annealing, and after additional 6 passes conditions, are shown in Fig. 5. Since work-softening was observed in both the 1-step aged (with approximately 40% untransformed supersaturated α' phase) and the intermediate annealed (with no untransformed α' left) Zn–Al alloy specimens, the possibility of softening by phase transformation ($\alpha' \rightarrow \alpha + \beta$) is ruled out. As such, the remaining possibility of properly explaining the work-softening phenomenon lies in the DRV/DRX-induced softening mechanism. Similar observation of work-softening during elevated-temperature ECAE has been reported by Purcek et al. [12, 13] in a couple of Zn–Al alloys and by Komura et al. [14] in an Al-Mg-Sc alloy. In their studies, some hardening was often observed in the first pass of ECAE, and with successive passes, an observed decrease in the extrusion load with the number of passes is attributed to the DRV/DRX due to high temperature extrusion during ECAE.

It would be appropriate at this point to differentiate between the softening effects of DRV and DRX. Theoretically, DRV produces no observable softening; rather a gradual balance of the hardening mechanisms (accumulation of dislocations) reaching eventually a stationary flow stress at large strains is observed. DRX, on the other hand, produces observable softening in dynamic conditions after a critical amount of hardening due to the accumulation of dislocations. Since recrystallization nucleates at points of high-lattice-strain energy, such as in areas close to grain boundaries, the grain refinement by an earlier DRX accelerates the nucleation rate of the following DRX. In this regard, an increasing DRX-induced softening will, at some point, surpass the work hardening to result in an overall work-softening behavior. According to this DRX-induced softening mechanism, an increase in the deformation strain by hot working (such as the initial 4-pass and the later 6-pass ECAE) enhances the reactions of DRX and results in the work-softening behavior in the Zn–Al alloy. The same theory would predict that a grain coarsening heat treatment, such as the applied intermediate annealing, will slow down the nucleation rate of DRX, depress the corresponding DRX-induced softening effect, and thus produce a special anneal-hardening behavior.

The effect of grain size

Since the microstructural evolution upon ECAE is difficult to resolve in the ultra-fine-grained 1-step aged Zn–Al alloy, it is being examined by using a 2-step aged (−10 °C/24 h + 250 °C/24 h) Zn–Al alloy with a relative coarser grain structure instead. Microstructures of the 2-step aged Zn–Al alloy in conditions prior to the ECAE and after 2, 6, and 10 passes of ECAE at −10 °C are shown in Fig. 6. The recorded extrusion load versus ECAE passes are shown in Fig. 7. As can be seen in Fig. 6a, prior to the ECAE, the 2-step aged Zn–Al alloy exhibits an equiaxed dual-phase grain structure with an average grain size of about 3 μm. It was observed that, after 2 passes of ECAE at −10 °C, the original equiaxed grains were distorted and the elongated α and β grains started to break up and intermix by the shear deformation (Fig. 6b). The deformation microstructure

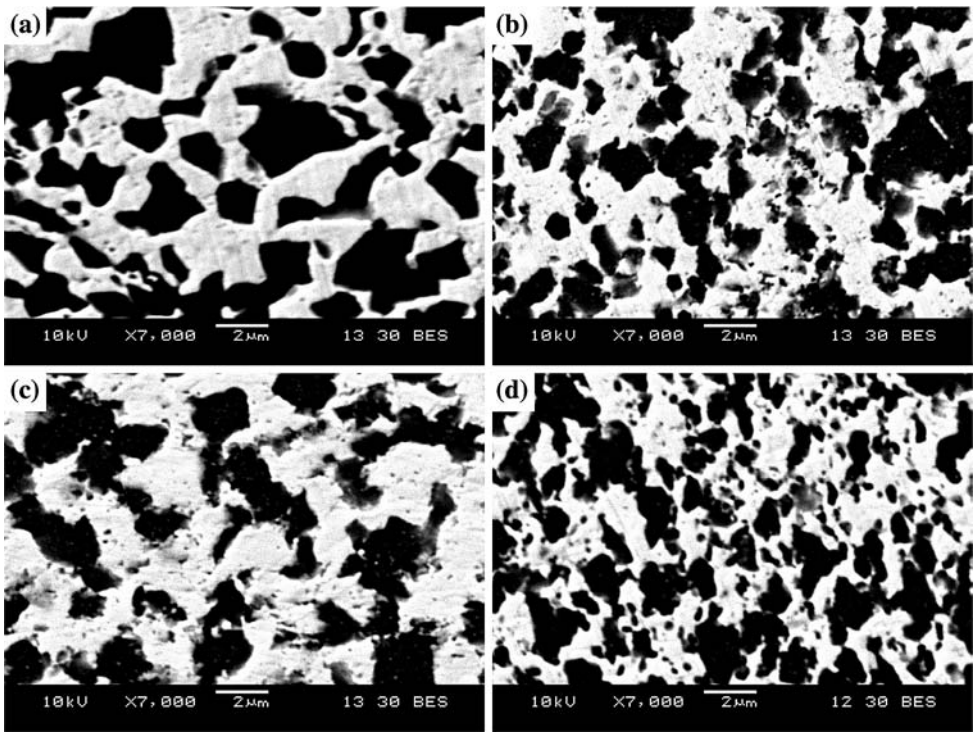

Fig. 6 Morphology of Zn-22 wt.% Al (**a**) 2-step aged (−10 °C/24 h + 250 °C/24 h), and ECAE for (**b**) 2 passes, (**c**) 6 passes, and (**d**) 10 passes at −10 °C

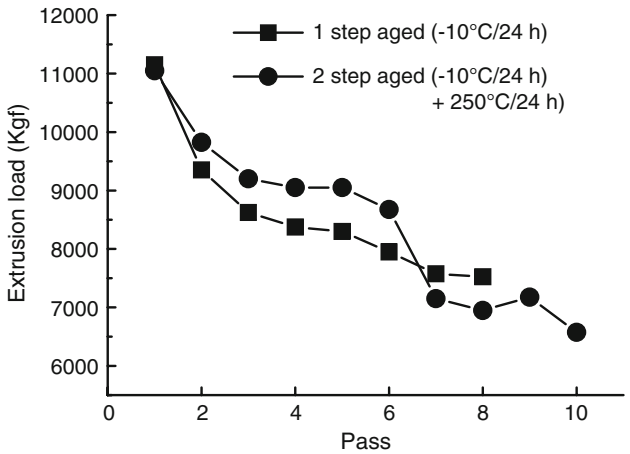

Fig. 7 Extrusion load versus ECAE pass in 1-step and 2-step aged Zn-22 wt.% Al alloy specimens

reveals the presence of many fine broken α chips (dark color) embedded in β grains (white color) and fine broken β chips in α grains due to intermixing. Accompanying these microstructural changes, a significant reduction in the extrusion load (i.e., work-softening) was recorded. Since the ECAE was performed at a temperature near the recrystallization temperature of the Zn-rich β phase, it is reasonable to assume that the work-softening arose from the occurrence of DRX in the β phase of the Zn–Al alloy and that fine β chips are likely to contribute very effectively to the softening.

A comparison of extrusion load versus ECAE pass curve of the 1-step aged (fine-grained, d ≈ 0.3 μm) Zn–Al alloy with that of the 2-step aged (coarse-grained, d ≈ 3 μm) Zn–Al alloy is shown in Fig. 7. As can be been in the figure, work-softening during −10 °C ECAE took place in both fine-grained and coarse-grained Zn–Al alloys, and the extrusion loads of the coarse-grained Zn–Al alloy were generally greater than those of the fine-grained alloy in the initial 6 passes of ECAE, but became equivalent to or even smaller than those of the fine-grained alloy in the later passes of ECAE when sufficient amounts of fine β grains were produced. It is evident, by correlating the increase of the amount of ultra-fine grains formed by mechanical deformation (Fig. 6) to the reduction in extrusion load of the alloy (Fig. 7), that this work-softening behavior is closely related to the increase of grain boundary areas (or to the reduction in grain size). Consequently, the most probable cause of work-softening, i.e., the DRX, must then be grain size or be grain boundary sensitivity. This argument about a coarse microstructure being harder than a finer microstructure can well explain the anneal-hardening introduced in the previous section. It has been reported in many severe plastic deformation studies that, accompanying the observed decrease in extrusion load with increasing number of passes, a remarkable increase in ductility is achieved through the SPD processing. Valiev et al. [15] attributes the increase in ductility during ECAE to the refinement of microstructure and to an increase in the fraction of high-angle grain boundaries, which results in the activation of boundary sliding and grain rotation deformation mechanism. Purcek [12], on the other hand, proposes that the increase in ductility may arise from the occurrence of dynamic

recovery and recrystallization due to high temperature pressing during ECAE. In either case, the observed extensive increase in ductility during ECAE leads to the speculation that, through a progressive work-softening processing, the alloy of interest will eventually exhibit HSR superplastic behaviors.

Superplasticity in the work-softened Zn–Al alloy

RT (25 °C) superplasticity tests were carried out on two sets of work-softened Zn-22 wt.% Al alloy specimens: one ECAEed for 8 passes at −10 °C and the other at 50 °C. The logarithmic plots of stress versus strain rate of these two sets specimens are shown in Fig. 8a. Values of strain rate sensitivity (m) determined from the derivatives of the polynomial fitted curves of Fig. 8a are plotted in Fig. 8b as a function of strain rate. The highest m values, i.e., indications of the best superplasticity, obtained in the Zn–Al alloys work softened (ECAEed) at −10 °C and 50 °C are 0.4 and 0.6, respectively, both of which occurred at a strain rate near 1×10^{-2} s^{-1}.

The RT tensile elongation data of the two Zn–Al alloys work softened at −10 °C and 50 °C, as plotted in Fig. 8c against strain rate, exhibited maximum elongations of 180% and 250%, respectively, both at a strain rate of 1×10^{-2} s^{-1}, indicating a RT HSR superplastic behavior in these two work-softened alloys. It is shown in Fig. 8c that the tensile elongation data of the Zn–Al alloy work softened at 50 °C are generally greater than those of the Zn–Al alloy work softened at −10 °C in the strain rate range investigated. In order to determine whether or not the grain boundary sliding or grain rotation mechanisms play a key role in the RT HSR in the Zn–Al alloy, line scratch tests and fracture surface examinations in search of characteristics of grain boundary sliding or grain rotation were carried out. The results show that there are no detectable off-set of line scratches found at grain boundaries nor pores formed at the triple junctions of grains to support the GBS or the grain rotation mechanisms being responsible for the RT HSR in the Zn–Al alloy. Thus, the extensive ductility, at HSR condition, achieved through a work-softening ECAE process appears to arise from the occurrence of DRX in the β phase of the Zn–Al alloy.

Conclusions

1. Having a recrystallization temperature of −7.5 °C, microduplex Zn-22 wt.% Al alloy exhibits a special DRX-induced work-softening behavior at RT.
2. The DRX-induced work-softening behavior can be enhanced by the reduction of grain size. As such, the application of a grain coarsening heat treatment on the fine-grained Zn–Al alloy will depress the nucleation rate of DRX and thus produce a special anneal-hardening behavior in the alloy.
3. An important discovery regarding the grain boundary-sensitive DRV has been made such that, through a

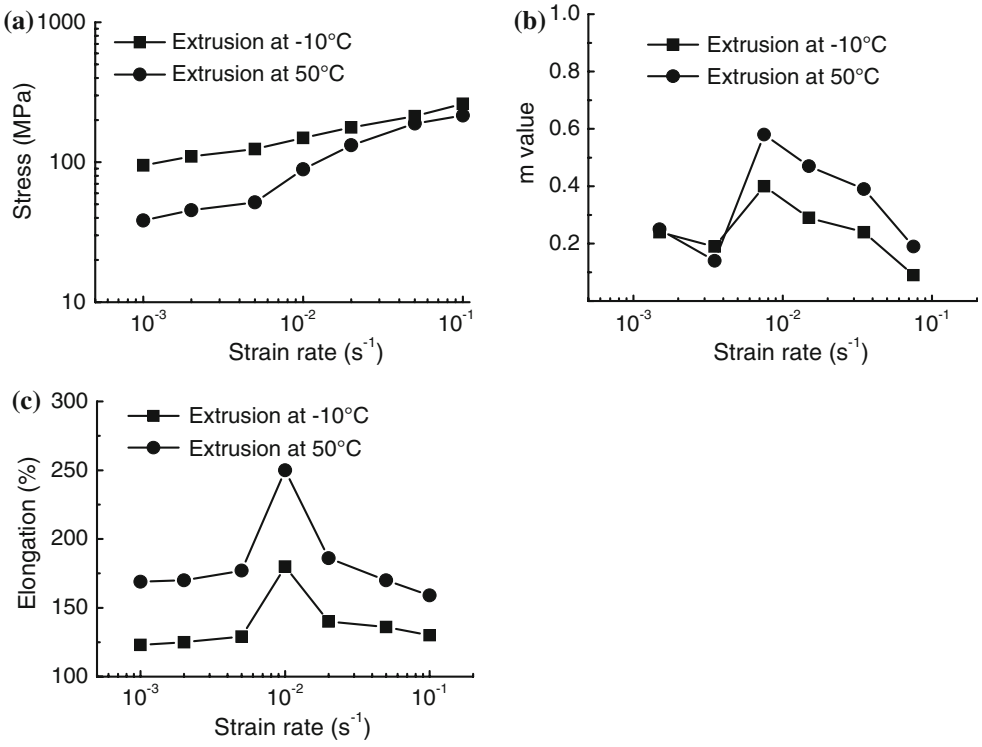

Fig. 8 (**a**) The logarithmic plot of RT tensile stress, (**b**) Variation of RT strain rate sensitivity, and (**c**) Variation of RT tensile elongation versus strain rate of Zn-22 wt.% Al alloy ECAEed 8 passes at −10 °C and 50 °C

progressive work-softening process, the Zn–Al alloy will eventually exhibit HSR superplastic behaviors.

Acknowledgement The authors gratefully acknowledge the financial support for this research by the National Science Council of R.O.C. under contract NSC 95-2221-E-036-029.

References

1. Casolco SR, Parra ML, Torres-Villasenor G (2006) J Mater Process Technol 174:389. doi:10.1016/j.jmatprotec.2005.02.271
2. Kaibyshev R, Avtokratova E, Apollonov A et al (2006) Scr Mater 54:2119. doi:10.1016/j.scriptamat.2006.03.020
3. Nikulin I, Kaibyshev R, Sakai T (2005) Mater Sci Eng A 407:62. doi:10.1016/j.msea.2005.06.014
4. Watanabe H, Ishikawa K, Mukai T (2007) Key Eng Mater 340–341:107
5. Lee CJ, Huang JC (2006) Mater Trans 47:2773. doi:10.2320/matertrans.47.2773
6. Beyerlein IJ, Alexander DJ, Tome CN (2007) J Mater Sci 42:1733. doi:10.1007/s10853-006-0906-x
7. Saravanan M, Pillai RM, Pai BC et al (2006) Bull Mater Sci 29:679
8. Kumar P, Xu C, Langdon TG (2006) Mater Sci Eng A 429:324. doi:10.1016/j.msea.2006.05.044
9. Tanaka T, Watanabe H, Kohzu M et al (2004) Mater Sci Forum 447–448:489
10. Huang WH, Yu CY, Kao PW et al (2004) Mater Sci Eng A 366:221. doi:10.1016/j.msea.2003.08.033
11. Staszewski M, Wesolowski J, Morawiec H (1996) Z Metallk 87:144
12. Purcek G (2005) J Mater Process Technol 169:242. doi:10.1016/j.jmatprotec.2005.03.012
13. Purcek G, Altan BS, Miskioglu I et al (2004) J Mater Process Technol 148:279. doi:10.1016/j.jmatprotec.2004.02.010
14. Komura S, Furukawa M, Horita Z et al (2001) Mater Sci Eng A 297:111. doi:10.1016/S0921-5093(00)01255-7
15. Valiev RZ, Alexandrov IV, Zhu YT et al (2002) J Mater Res 17:5. doi:10.1557/JMR.2002.0002